

# Adsorption of pollutants from rainwater: An efficient combination of fly ash and activated carbon

Anna Marszałek, Ewa Puszczalo\*, Mariusz Dudziak

Silesian University of Technology, Faculty of Energy and Environmental Engineering, Konarskiego 18, 44-100 Gliwice, Poland

\* Corresponding author, e-mail:  
[ewa.puszczalo@polsl.pl](mailto:ewa.puszczalo@polsl.pl)

Presented at  
MEMSEP & PERMEA 2025  
15th International Conference  
on Membrane and Separation  
Processes & 10th Membrane  
Conference of Visegrad Countries,  
24–26 June, 2025, Chorzów, Poland.  
Guest Editor: Maciej Szwałt.

## Article info:

Received: 30 May 2025  
Revised: 12 September 2025  
Accepted: 18 November 2025

## Abstract

This study explores the use of waste materials such as activated fly ash (AP1) and its mixture with activated carbon (AP2) for rainwater treatment. The adsorption of heavy metals (Ni, Pb, Cu) and bisphenol A (BPA) was tested under varying adsorbent doses, contact times, and solution pH. Fly ash was chemically activated with NaOH, while activated carbon was obtained from spent filter cartridges and similarly treated. Both adsorbents were characterized for surface area, porosity, pore size distribution, and point of zero charge. Activation significantly increased the surface area of fly ash and combining it with activated carbon further improved adsorption performance. AP2 showed the highest removal efficiencies, indicating a synergistic effect of the two materials. The results demonstrate the potential of reusing industrial and municipal waste in rainwater treatment, supporting sustainable development and circular economy practices.

## Keywords

fly ash, activated carbon, adsorption, bisphenol A, heavy metals

## 1. INTRODUCTION

In recent years, there has been growing interest in developing modern adsorbents with high efficiency for removing pollutants from water, including rainwater. Waste materials are particularly important in this context, as they exhibit good sorption properties and align with the principles of a circular economy (Dehghani et al., 2023; Othmani et al., 2022).

Fly ash, a by-product of coal combustion in power plants, is one of the most widely used industrial wastes (Alterary and Marei, 2021; Bhatt et al., 2019; Yao et al., 2015). Its high specific surface area, porosity and reactive aluminosilicate compounds make it an effective adsorbent for heavy metals and organic pollutants in aqueous solutions (Aigbe et al., 2021; Hosseini Asl et al., 2019). In addition, its sorption capacity can be further enhanced through chemical, physical, or thermal activation (Gong et al., 2019; Katara et al., 2013).

The second waste material considered in this study is activated carbon from household jug filters. These filters, commonly used in households, contain ion exchange resin and activated carbon (Szymańska and Nowicki, 2019). The average consumer uses six to twelve filters per year, representing a significant source of reusable adsorbent material (Szymańska and Nowicki, 2019). To date, only a limited number of studies have explored the reuse of this type of waste in rainwater treatment.

Combining activated fly ash with used activated carbon can be particularly beneficial in urban areas, where rainwater runoff is a major source of pollution (Zhang and Husain, 2021).

This approach can relieve the burden on urban wastewater treatment plants and reduce the environmental impact of urbanisation. Additionally, reusing these materials represents a sustainable and rational waste management strategy (Mush-taq et al., 2019).

The purpose of this study was to experimentally investigate the efficiency of the removal of selected pollutants (nickel, lead, copper, and bisphenol A) from rainwater using activated fly ash and its mixture with waste activated carbon. The study included physicochemical analysis of rainwater samples, adsorbent characterisation, and evaluation of adsorption efficiency as a function of adsorbent dose, contact time, and solution pH.

## 2. MATERIALS AND METHODS

### 2.1. Methodology of adsorbent preparation

The study used fly ash taken from the New Jaworzno Power Plant Branch in Jaworzno and activated carbon from tap water filter cartridges from a popular company on the Polish market.

Fly ash was activated by mixing it with a 10 M NaOH solution in a weight ratio of 1:1, according to procedures described in the literature (Oktaviansyah et al., 2024). The mixture was mixed with a mechanical stirrer for 15 minutes, then placed in heat-resistant silicone moulds and dried in a laboratory dryer at 60 °C for 24 hours to cure. The resulting material was crushed in a mortar and washed with distilled water to remove excess unreacted NaOH. The mixture was then



dried again at 105 °C for 12 hours. A fraction with a grain size of 0.2–0.5 mm was obtained by pneumatic sieving. This adsorbent was designated AP1. A second AP2 adsorbent was prepared in a similar manner, in which fly ash was mixed with activated carbon spent from household jug filters in a weight ratio of 5:1. To add the activated carbon, the spent filter medium was first subjected to drying at 105 °C for 12 hours. After drying, the activated carbon was mechanically separated from the ion exchange resin (Fig. 1).

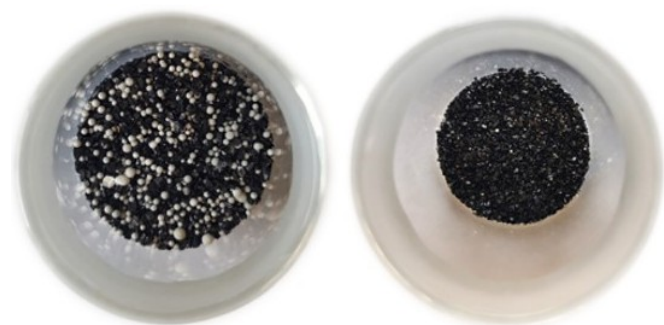


Figure 1. Filling of the filter cartridge before and after separation of the ion exchange resin (own photo).

The activated carbon was then crushed in a mortar. The ash/carbon mixture was subjected to an activation identical to AP1. The purpose of adding the waste activated carbon was to reuse it and increase the adsorption efficiency of the composite, in line with the concept of a circular economy.

## 2.2. Characteristics of adsorbents

The pore structure of the samples was characterised by the volumetric low-pressure nitrogen adsorption (LPNA) method on the ASAP 2020 analyser (Micromeritics). The nitrogen adsorption isotherms were determined under controlled pressure conditions in the range of 0–0.1 MPa and a temperature of 77 K. Based on nitrogen isotherms, the specific surface area was determined assuming monolayer Langmuir model (Langmuir, 1918) and multilayer BET model (Brunauer et al., 1938) filling of adsorbate molecules, micropore volume DFT model (Olivier, 1995), and pore size distribution (DFT model).

The zero charge point was measured using the suspension method (Sulyman et al., 2021). For this purpose, 100 mg of adsorbent was added to 100 ml of distilled water with an initial pH in the range of 2 to 10. The suspensions were stirred at 25 °C for 24 hours. After this time, the final pH of the solutions was measured. The difference between the initial and final pH values ( $\Delta\text{pH} = \text{pH}_f - \text{pH}_i$ ) for each series was plotted as a function of  $\text{pH}_i$ . The pH of pzc was then estimated at the point where it crossed  $\Delta\text{pH} (\text{pH}_i - \text{pH}_f) = 0.0$ . The pH adjustment was performed using 0.1 mol/L  $\text{HNO}_3$  or NaOH solution.

## 2.3. Subject of research

The subject of the study was rainwater collected from the metal roof of a single-family building. Physicochemical parameters such as pH, conductivity, colour, total hardness, UV absorbance at 254 nm, phenolic index and metal concentrations were determined in the analysed sample: Zn, Cu, Ni, Pb, Mn and Fe. The results are summarised in Table 1, together with the allowed values (Regulation, 2019).

Table 1. Physico-chemical parameters of the tested rainwater.

Parameter	Unit	Rainwater	Norm (Regulation, 2019)
pH	–	6.25	6.50–9.00
Conductivity	$\mu\text{S}/\text{cm}$	56.90	–
Colour	$\text{mgPt}/\text{L}$	87.00	–
Hardness og.	$\text{mval}/\text{L}$	0.50	–
Zinc		0.47	2.00
Copper	$\text{mg}/\text{L}$	0.03	0.50
Nickel		0.18	0.50
Lead		0.07	0.10
Phenolic index		0.32	0.1

The presence of phenols in rainwater can be explained by the location of the building from which the sample was taken – there are industrial plants nearby. Phenolic compounds are deposited on the roof surface and then enter the drain with rainwater (De Buyck et al., 2021).

## 2.4. Adsorption methodology

The prepared adsorbents were used to remove selected pollutants from rainwater. For this purpose, model aqueous solutions were prepared. Selected heavy metals were added to the actual rainwater sample, obtaining a concentration of 2 mg/L: copper (Cu), lead (Pb) and nickel (Ni) – designated as sample WO1 – and bisphenol A with a concentration of 1 mg/L – designated as sample WO2.

The aim of the study was to determine the removal efficiency of heavy metals and organic compounds (bisphenol A as an example) from rainwater. Adsorption studies were conducted in a static system in 100 mL glass bottles, on a mechanical shaker at 320 rpm.

The influence of the following process parameters on adsorption efficiency was analysed:

- adsorbent dosage (1–8 g/L),
- contact time (10–180 min. for Cu, Pb, Ni, and 60–360 min. for BPA)
- pH of the solution (2–10).

The volume of solution in each experiment was 50 mL. When studying the effect of the adsorbent dose, the contact time was 60 minutes. In contrast, when studying the effect of contact time and solution pH, a constant adsorbent dose of 6 g/L (i.e. 0.03 g per 50 mL) was used. The concentration of BPA after the adsorption process was calculated using the Beer-Lambert formula based on calibration with standards of known BPA concentration. BPA shows characteristic absorption at 275 nm, which allows its detection. Metal concentration determinations were performed using Merck assays.

Reagents used in research:

Copper standard solution 1000 mg Cu ( $\text{CuCl}_2$  in  $\text{H}_2\text{O}$ ) Titrisol<sup>®</sup> from Merck KGaA (Germany). Lead standard solution 1000 mg Pb lead solution ( $\text{Pb}(\text{NO}_3)_2$  in  $\text{H}_2\text{O}$ ) from Merck (Germany). Nickel standard solution 1000 mg Ni ( $\text{NiCl}_2$  in  $\text{H}_2\text{O}$ ) Titrisol<sup>®</sup>, from Merck (Germany).

All adsorption experiments were performed in triplicate, and the results showed very good reproducibility (standard deviation did not exceed 3 % of the mean values).

Table 2. Summary of structural properties of adsorbents.

Adsorbent	BET surface area [ $\text{m}^2/\text{g}$ ]	DFT total micropore volume [ $\text{cm}^3/\text{g}$ ]	Langmuir surface area [ $\text{m}^2/\text{g}$ ]	Pore size [nm]
Fly ash before activation (FA)	3.25	0.00	10.70	7.42
Waste activated carbon (AC)	1 465.10	0.65	2 215.40	2.52
Fly ash after activation (AP1)	36.80	0.03	66.20	2.18
Fly ash with carbon after activation (AP2)	153.90	0.07	237.90	4.97

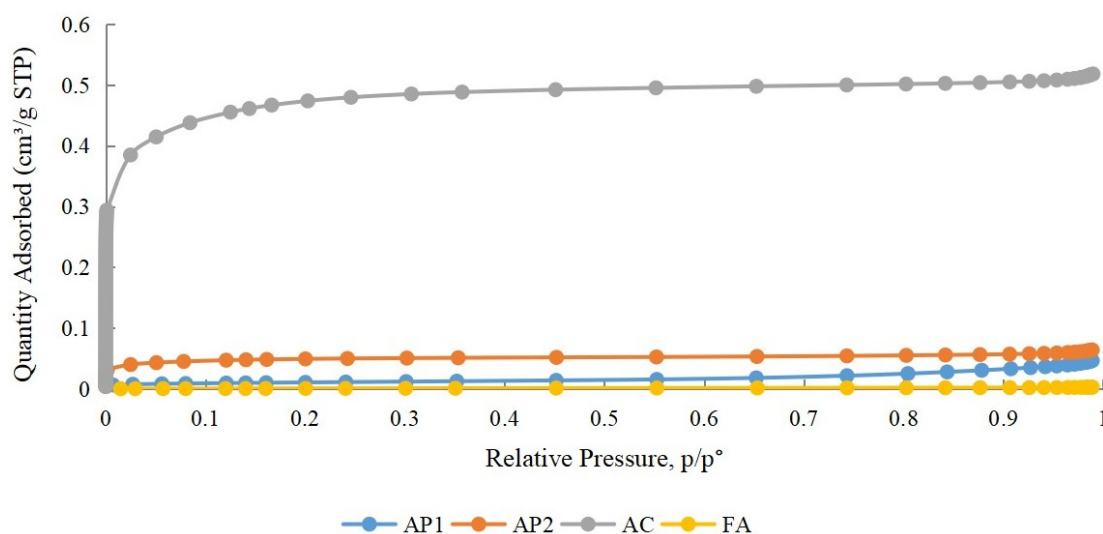


Figure 2. Dependence of adsorbed quantity on relative pressure.

## 2.5. Adsorption Kinetics

The adsorption kinetics was evaluated using the pseudo first and pseudo second order models. The calculation of kinetic parameters was performed following the procedures described in our previous study (Marszałek, 2022), using linearized forms of the models.

## 3. RESULTS AND DISCUSSION

### 3.1. Characteristics of adsorbent

The structural properties of the adsorbents were measured to better understand their potential to remove pollutants from rainwater. These properties include specific surface area, porosity and pore size distribution, which have a significant impact on adsorption efficiency (Table 2, Fig. 2, 3).

The results of the specific surface area (SSA) measurements for the prepared adsorbents indicate a significant influence of both the activation process and the modification of the fly ash by the addition of waste activated carbon. For sample FA, the

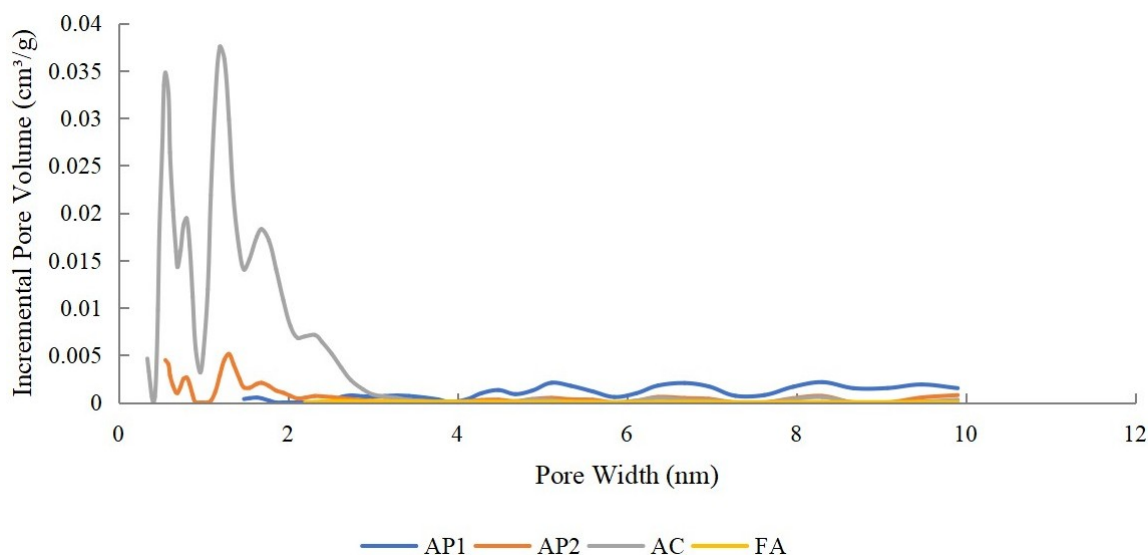


Figure 3. Dependence of pore volume per specific pore diameter interval.

specific surface area of approximately  $3.5 \text{ m}^2/\text{g}$  is relatively low, suggesting that the fly ash without activation has limited adsorption capacity. Sample AP1, after activation, shows a significantly higher specific surface area of up to  $36 \text{ m}^2/\text{g}$ , which is more than a 10-fold increase compared to sample FA. This increase in surface area is the result of the activation applied, which opens up additional micropores in the fly ash structure, improving its ability to adsorb contaminants. A similar increase in the specific surface area is observed in sample AP2, which reached a surface area of almost  $154 \text{ m}^2/\text{g}$  when waste activated carbon of  $1465 \text{ m}^2/\text{g}$  was added to fly ash.

The phenomenon of a fourfold increase in specific surface area after the addition of activated waste carbon in sample AP2 is an interesting result that suggests that activated waste carbon can be an effective support material in adsorption processes. Furthermore, activated carbon, known for its high specific surface area and adsorption capacity, could work with fly ash

to improve its effectiveness in the removal of contaminants (Tan et al., 2017).

The zero charge point ( $\text{pH}_{\text{PZC}}$ ) of the adsorbents was measured using the slurry method. Figure 4 shows the results of the zero charge point measurement for both adsorbents.

The  $\text{pH}_{\text{PZC}}$  values of the adsorbents used were read from the graphical data. For adsorbent AP1, the  $\text{pH}_{\text{PZC}}$  value is 9.2 for AP2 9.3, suggesting that at a solution pH below this value, the surface of the adsorbent gains a positive charge. In practice, this means that under such conditions they can adsorb anionic ions more efficiently, which will be attracted to the positively charged surface. However, when the pH of the solution exceeds the  $\text{pH}_{\text{PZC}}$  value, the adsorbents will assume a negative charge, which favours the adsorption of cations, which will be attracted to a negatively charged surface (Zaimee et al., 2012).

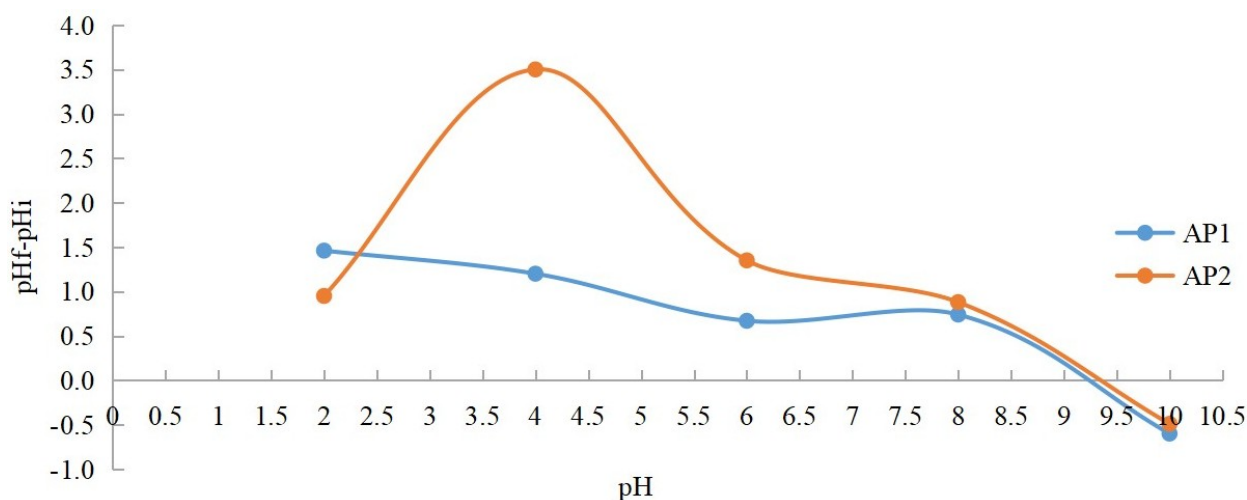


Figure 4. Measurement of the zero charge point of the adsorbents.

### 3.2. Time- and dose-dependent adsorption efficiency of heavy metals from rainwater

Figures 5 and 6 show the effect of the adsorbent dose on the removal efficiency of Ni(II), Cu(II), and Pb(II) ions from rainwater for AP1 and AP2, respectively.

The use of AP2 adsorbent, a combination of activated fly ash and spent activated carbon, showed significantly higher heavy metal removal efficiency compared to AP1, especially at lower doses of adsorbents (1–2 g/L). The presence of activated carbon significantly improved the adsorption properties of the material, confirming the effectiveness of such a modification.

The most noticeable difference between the two materials was in the adsorption of nickel ions. At a dose of 1 g/L, AP2 removed nearly twice as many Ni(II) ions as AP1. In the case of lead Pb(II), both adsorbents showed very high efficiencies, but here AP2 also achieved full removal of the contaminant (100%) already at a dose of 4 g/L, making it an extremely effective material. When considering a dose of 4 g/L, the heavy metal adsorption for AP2 was successively Ni(II) 64%, Cu(II) 89%, Pb(II) 100%. To further investigate the adsorption behaviour over time, the effect of contact time on the amount of adsorbed Ni(II), Cu(II), and Pb(II) ions for both AP1 and AP2 is presented in Figure 7. These graphs allow for a direct comparison of the adsorption kinetics of the two materials and highlight the rate at which equilibrium is reached for each metal ion under the tested conditions.

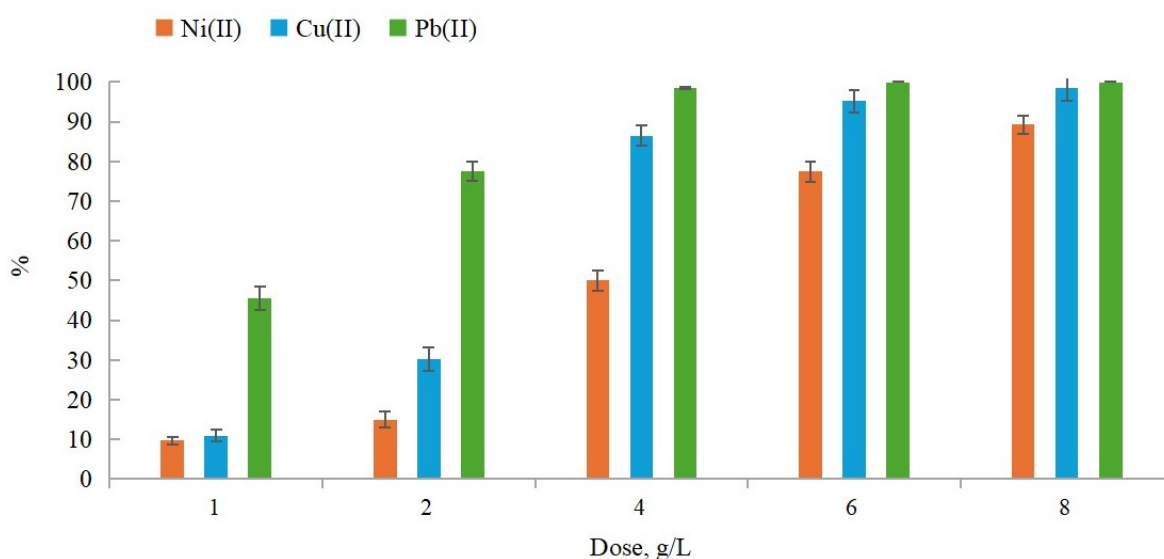


Figure 5. Effect of AP1 adsorbent dose on the removal efficiency of Ni (II), Cu (II) and Pb (II) ions from rainwater (static adsorption, solution volume: 50 cm<sup>3</sup>, contact time: 60 min). Data are presented as mean  $\pm$  SD ( $n = 3$ ).

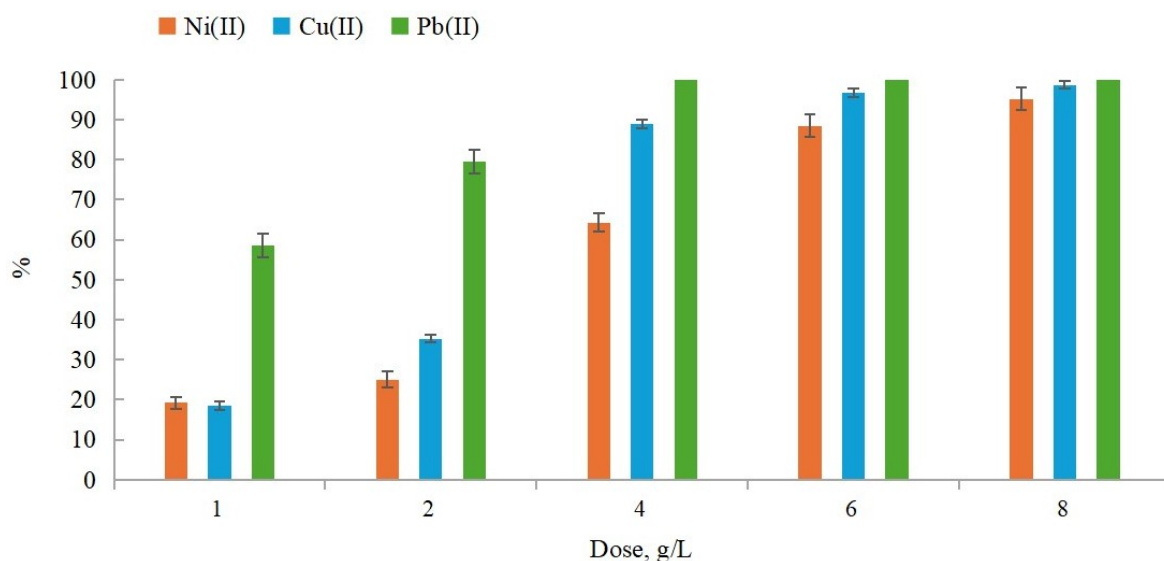


Figure 6. Effect of AP2 adsorbent dose on the removal efficiency of Ni (II), Cu (II) and Pb (II) from rainwater (static adsorption, solution volume: 50 cm<sup>3</sup>, contact time: 60 min). Data are presented as mean  $\pm$  SD ( $n = 3$ ).

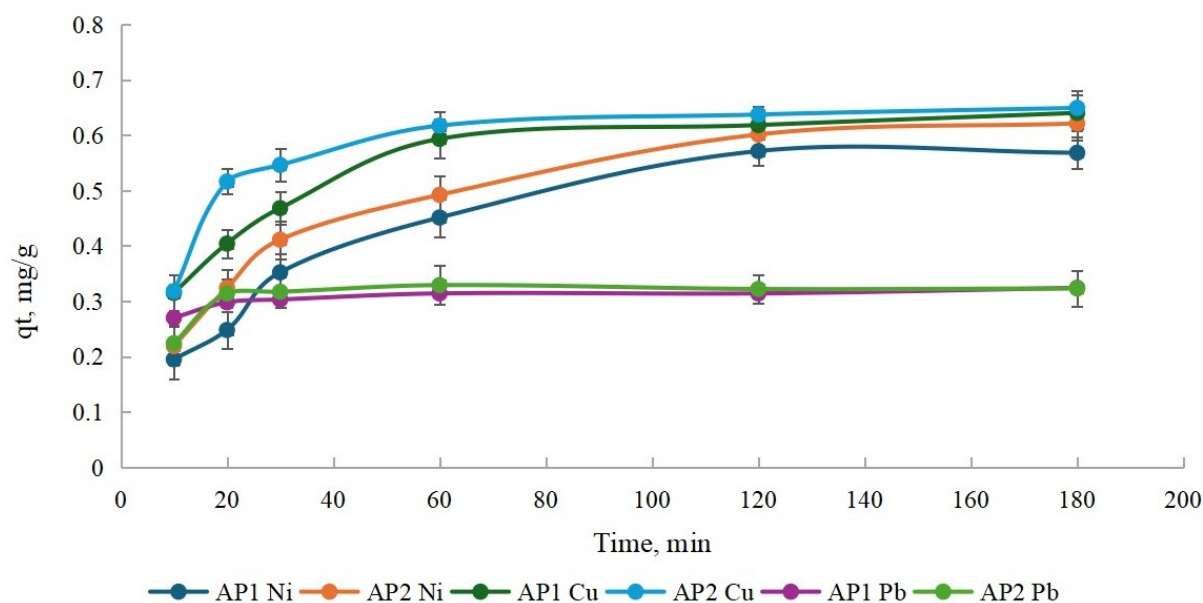


Figure 7. Effect of contact time on the amount of adsorbed Ni(II), Cu(II) and Pb(II) ions by AP1 and AP2 adsorbents. Data are presented as mean  $\pm$  SD ( $n = 3$ ).

In the case of nickel ions, there is a clear increase in  $q_t$  values over time for both adsorbents, with AP2 reaching slightly higher maximum values. The highest adsorption intensity occurs in the first 30 minutes, after which the process stabilises. A similar trend was observed for copper (Cu), where AP2 also shows a higher adsorption capacity than AP1. For lead, irrespective of the type of adsorbent, the adsorption curves are almost flat – this means that the equilibrium state is reached quickly and the variation of  $q_t$  values over time is low.

In connection with the research presented here, information was collected on the effectiveness of different waste materials used as adsorbents in removing heavy metals from water under laboratory conditions (Table 3). The data show the effectiveness of the different materials because of their different physico-chemical properties. This compilation allows for an assessment of the potential of using waste materials as low-cost and environmentally friendly solutions in water treatment processes.

Both NaOH-activated fly ash and activated carbon are chemically stable materials, resistant to dissolution and structural damage in aqueous environments. Although detailed regeneration tests were not included in the present study, reports in the literature indicate that alkali-activated fly ash can be effectively regenerated by simply washing or mild thermal treatment, with only a slight decrease in adsorption efficiency after several cycles (Guo et al., 2024; Singh et al., 2022). Activated carbon is also well known for its reusability through chemical or thermal regeneration, which supports its sustainable application in adsorption-based processes (Gkika et al., 2022). Therefore, the investigated composite adsorbent (AP2) can be considered a promising material in terms of high adsorption.

Table 3. Comparison of the effectiveness of different waste materials used as adsorbents in the removal of heavy metals from water under laboratory conditions.

Waste material	Metal removed	Adsorption efficiency	Source
Fly ash with waste activated carbon of NaOH modified (AP2)	Pb(II)	100%	This work
	Cu(II)	89.0%	
	Ni(II)	64.0%	
Fly ash of NaOH modified (AP1)	Pb(II)	98.5%	This work
	Cu(II)	86.0%	
	Ni(II)	50.0%	
Activated carbon from sewage sludge	Cu(II)	97.0%	Guo et al. (2017)
Peanut shell biochar	Cd(II)	99.7%	Cobbina et al. (2019)
	Hg(II)	99.5%	
	Pb(II)	99.1%	
Activated carbon from sewage sludge modified with fly ash	Cu(II)	99.6%	Mao et al. (2024)
	Cd(II)	99.7%	
Fly ash	Cu(II)	91.4%	Alinnor (2007)
	Pb(II)	77.6%	
Modified fly ash (MSWI)	Pb(II)	90.0%	Qiu et al. (2018)
	Cu(II)	70.0%	
	Ni(II)	40.0%	
Fly ash of KOH modified	Cr(II)	97.5%	Jiang et al. (2019)

### 3.3. Time- and dose-dependent adsorption efficiency of bisphenol A from rainwater

Figure 8 show the effect of adsorbent dose on the removal efficiency of BPA from rainwater for AP1 and AP2, respectively.

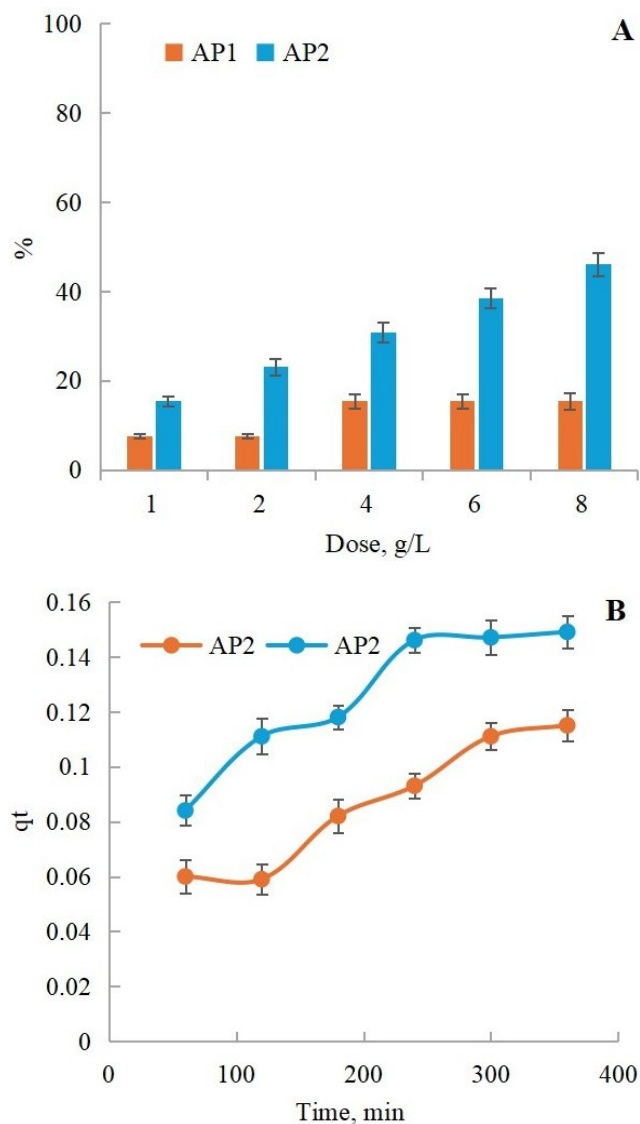


Figure 8. Effect of adsorbent dose on bisphenol adsorption efficiency (A) and bisphenol adsorption kinetics (qt) as a function of time (B) for samples AP1 and AP2. Data are presented as mean  $\pm$  SD ( $n = 3$ ).

Analysis of the bisphenol adsorption efficiency of the two types of adsorbents, AP1 and AP2, showed clear differences in their effectiveness. According to the results, the adsorption efficiency increased with increasing adsorbent dose only in the case of the AP2 sample. At the highest dose, i.e., 8 g/L, AP2 reached an efficiency of 46.15%, while AP1 remained constant at 15.38% from as low as 4 g/L, which may indicate saturation of the sorption surface or lower adsorption activity of this material. In the adsorption kinetics graph, it can be

seen that AP2 reached much higher adsorption values in a shorter time and showed a more stable increase in the amount adsorbed over time compared to AP1. AP2 reached a value close to 0.16 mg/g after 360 minutes, while AP1 only reached about 0.11 mg/g. The curve for AP2 indicates a rapid initial phase of adsorption (up to about 100 minutes), followed by a stabilisation phase. For AP1, the rate of adsorption was lower and the growth curve was more gradual. These data confirm that the AP2 sample, containing activated carbon, has a higher sorption capacity and bisphenol A removal efficiency than AP1. These findings indicate that the higher activated carbon content in AP2 provides a more favourable surface for BPA uptake, particularly due to the presence of aromatic domains that promote  $\pi$ - $\pi$  interactions.

### 3.4. Influence of solution pH on the performance of the adsorbent

Figure 9 presents the adsorption efficiencies of lead (A), copper (B), nickel (C), and bisphenol A (D) as a function of the pH of the solution for AP1 and AP2. The graphs highlight the influence of pH on the removal performance of both adsorbents and allow for a direct comparison of their efficiency toward metal ions and organic pollutants under varying acidic and alkaline conditions.

Investigation of the effect of pH on nickel and copper adsorption efficiencies showed that AP2 had very high adsorption efficiencies in a wide pH range (4–10), reaching a maximum of 81%, also AP1 reached similar values, i.e. 76.5%.

In acidic environments (pH 2), the adsorption efficiency of both samples decreased, probably due to the competition of  $H^+$  ions with Ni(II) and Cu(II) for active sites (Jiang et al., 2019). In contrast, Pb(II) adsorption remained high throughout the pH range studied, which may be related to its higher affinity for oxygen-containing functional groups and the formation of strong surface complexes, which is consistent with reports by other authors (Chowdhury et al., 2012). For bisphenol A (BPA), adsorption efficiency was much lower compared to metal ions, and was strongly dependent on the solution pH. For AP2, efficiency reached 35% at pH 2 and 33% at pH 6, but decreased sharply to 20% at pH 8 and below 10% at pH 10. AP1 showed even lower values under analogous conditions. This behaviour can be explained by the molecular properties of BPA. With two phenolic groups (pKa 9.6–10.2), BPA remains mostly in neutral form at low and moderate pH, where adsorption is mainly driven by hydrophobic interactions, hydrogen bonding and  $\pi$ - $\pi$  stacking with the carbonaceous surface (Tursi et al., 2018). As the pH increases towards alkaline values, BPA undergoes deprotonation, which enhances its solubility in water and leads to stronger electrostatic repulsion from the negatively charged surface, additionally reinforced by  $OH^-$  competition. This explains the sharp drop in removal efficiency at higher pH values (Amadou Kiari et al., 2024).

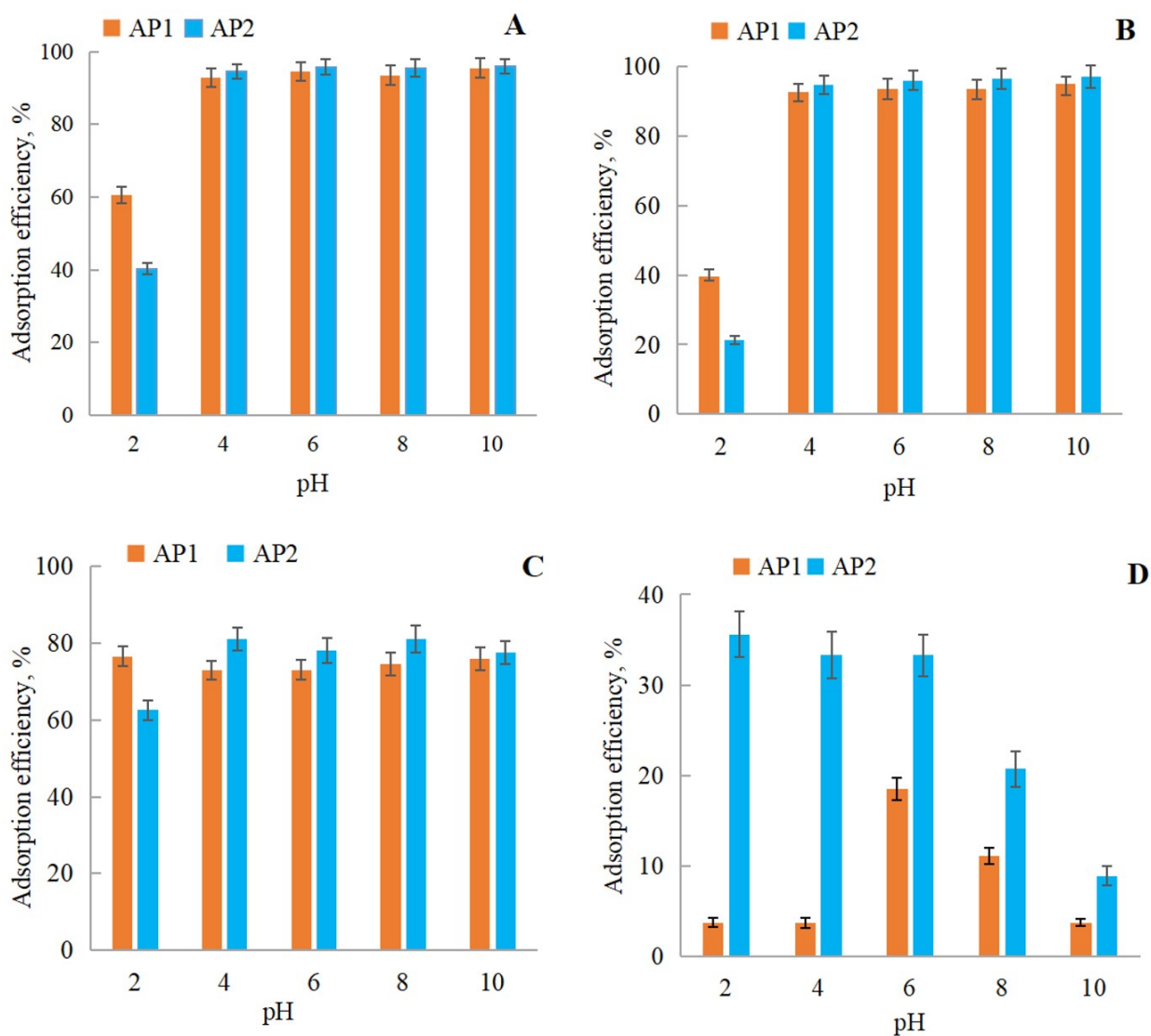


Figure 9. Adsorption efficiencies of lead (A), copper (B), nickel (C) and bisphenol A (D) as a function of solution pH for samples AP1 and AP2. Data are presented as mean  $\pm$  SD ( $n = 3$ ).

#### 4. ADSORPTION KINETICS

The adsorption kinetics of Ni, Pb, Cu and BPA on the two adsorbents (AP1 and AP2) was examined using pseudo-first order (PFO) and pseudo-second order (PSO) models, with the corresponding parameters presented in Table 4 and the fitted curves in Figure 10.

The pseudo-first order model showed good agreement for most systems, with correlation coefficients ( $R^2$ ) ranging from 0.93 to 0.99 for Cu(II), Ni(II) and Pb(II), indicating a relatively fast adsorption process. On the contrary, BPA exhibited a much lower fit ( $R^2 = 0.72$ – $2.82$ ), suggesting slower adsorption kinetics and weaker interaction with the surface. The pseudo-second order (PSO) model provided an excellent fit for all the studied adsorbates ( $R^2 = 0.89$ – $0.99$ ), particularly for Cu(II) and Pb(II) ( $R^2 = 0.99$ ), confirming that chemical interactions such as surface complexation and specific bind-

ing to oxygenated functional groups predominantly control the adsorption mechanism. The high correlation of PSO for Ni(II) and BPA ( $R^2 = 0.99$ ) also suggests the involvement of chemisorption, although diffusion effects may still contribute to the overall rate.

For AP2, the PFO model adequately described Cu(II) and Ni(II) adsorption ( $R^2 = 0.97$ – $0.99$ ), while Pb(II) and BPA showed weaker fits ( $R^2 = 0.72$ – $0.73$ ), consistent with slower uptake. The PSO model again achieved excellent agreement ( $R^2 = 0.89$ – $0.99$ ), especially for Cu(II) and Pb(II), indicating stronger surface interactions and possible electron exchange or exchange mechanisms. The relatively lower fit for BPA under the PSO model suggests a multistep adsorption process involving both chemisorption and intraparticle diffusion, in line with previously reported findings for phenolic compounds in carbonaceous materials (Aigbe et al., 2021; Guo et al., 2017; Mao et al., 2024).

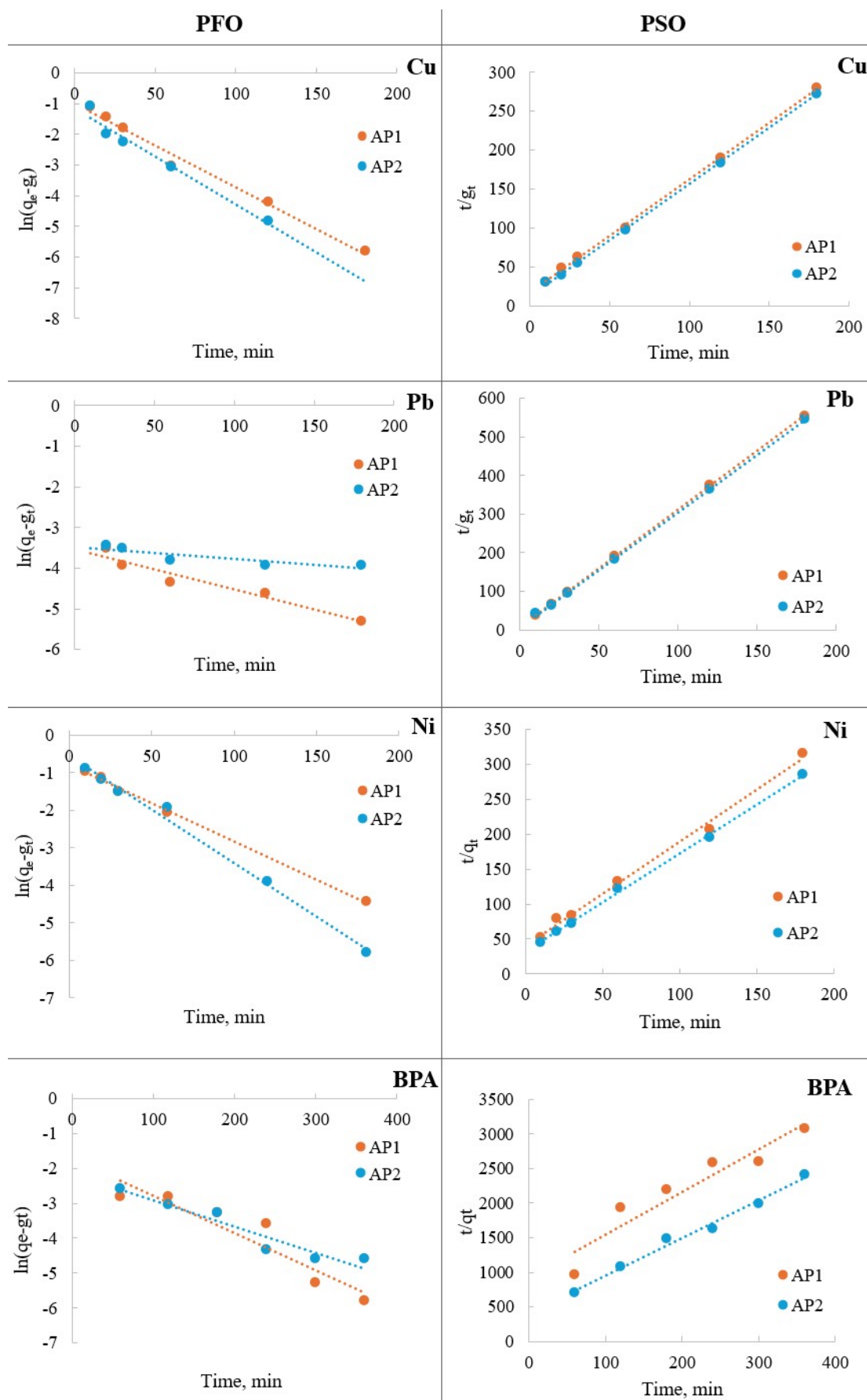


Figure 10. The adsorption kinetics of Ni, Pb, Cu, and BPA on the two sorbents (AP1 and AP2).

Table 4. Parameters of kinetic models (PFO, PSO) for the adsorption of Ni, Pb, Cu, and BPA onto AP1 and AP2.

PFO				PSO			
AP1							
Adsorbate	$K_1$ [1/min]	$q_e$ [mg/g]	$R^2$	Adsorbate	$q_e$ [mg/g]	$K_2$ [g/(mg·min)]	$R^2$
Cu	0.027	0.102	0.99	Cu	0.69	0.12	0.99
Pb	0.009	0.0004	0.93	Pb	0.33	1.49	0.99
Ni	0.020	0.162	0.99	Ni	0.72	0.059	0.99
BPA	0.016	0.040	0.82	BPA	0.18	0.076	0.99
AP2							
Cu	0.031	0.072	0.97	Cu	0.69	0.176	0.99
Pb	0.003	0.0003	0.73	Pb	0.34	1.341	0.99
Ni	0.029	0.282	0.99	Ni	0.67	0.055	0.99
BPA	0.012	0.026	0.72	BPA	0.16	0.042	0.89

## 5. SUMMARY

The purpose of the study was to evaluate the effectiveness of two adsorption materials – activated fly ash and activated fly ash combined with activated carbon of waste – in removing pollutants, including heavy metals and organic substances, from rainwater. The research carried out allowed one to formulate the following conclusions:

- An increase in adsorbent mass and contact time with the solution resulted in an increase in the amount of heavy metal ions (nickel, copper, lead) adsorbed in both materials tested.
  - Nickel: for AP1 adsorbent, dose of 0.4 g/50 mL, contact time 120 minutes; for AP2 adsorbent, dose of 0.3 g/50 mL, contact time 120 minutes.
  - Copper: 0.3 g/50 mL dose and 60 minutes contact time for both adsorbents.
  - Lead: for AP1 adsorbent, 0.2 g/50 mL dose rate and 60 minute contact time; for AP2 adsorbent, 0.2 g/50 mL dose rate and 20 minute contact time.
- The highest adsorption efficiency was observed for lead removal, reaching 100% efficiency, demonstrating high efficiency of both adsorbents in removing this metal.
- The use of AP2 adsorbent (a combination of fly ash and waste activated carbon) resulted in a 20 % increase in the efficiency of bisphenol A removal from rainwater, indicating the beneficial effect of activated carbon in improving the adsorption capacity of the material.
- The pH value had a significant effect on the adsorption efficiency of heavy metals and BPA, appropriate adjustment of the pH of the solution improved the adsorption efficiency. The favourable pH for heavy metal adsorption is in the slightly acidic to neutral range (pH 5–7), while for BPA it is in the acidic range (pH 2–6).

- The combination of activated fly ash with waste activated carbon proved to be a very favourable solution as it increased the adsorption efficiency of the pollutants. Activated carbon, due to its large specific surface area and ability to adsorb a wide range of contaminants, supports fly ash by improving its adsorption properties.

It should be noted that adsorption isotherm and adsorbent regeneration tests were not conducted in this study. These aspects should be addressed in future research to provide a more comprehensive understanding of the adsorption mechanism and the reusability potential of the tested materials.

## ACKNOWLEDGMENTS

*The research was financed by the statutory research fund of the Department of Water and Wastewater Engineering (08/040/BK\_25/0221).*

## REFERENCES

- Aigbe U.O., Ukhurebor K.E., Onyancha R.B., Osibote O.A., Darmokoesoemo H., Kusuma H.S., 2021. Fly ash-based adsorbent for adsorption of heavy metals and dyes from aqueous solution: a review. *J. Mater. Res. Technol.*, 14, 2751–2774. DOI: [10.1016/J.JMRT.2021.07.140](https://doi.org/10.1016/J.JMRT.2021.07.140).
- Alinnor I.J., 2007. Adsorption of heavy metal ions from aqueous solution by fly ash. *Fuel*, 86, 853–857. DOI: [10.1016/j.fuel.2006.08.019](https://doi.org/10.1016/j.fuel.2006.08.019).
- Alterary S.S., Marei N.H., 2021. Fly ash properties, characterization, and applications: a review. *J. King Saud Univ. Sci.*, 33, 101536. DOI: [10.1016/J.JKSUS.2021.101536](https://doi.org/10.1016/J.JKSUS.2021.101536).
- Amadou Kiari M.N., Konan A.T.S., Sanda Mamane O., Ouattara L.Y., Ibrahim Grema M.H., Siragi Dounounou Boukari M., Adamou Ibro A., Malam Alma M.M., Yao K.B., 2024. Adsorption kinetics, thermodynamics, modeling and optimization

- of bisphenol A on activated carbon based on *Hyphaene Thebaica* shells. *Case Stud. Chem. Environ. Eng.*, 10, 100903. DOI: [10.1016/j.cscee.2024.100903](https://doi.org/10.1016/j.cscee.2024.100903).
- Bhatt A., Priyadarshini S., Mohanakrishnan A.A., Abri A., Sattler M., Techapaphawit S., 2019. Physical, chemical, and geotechnical properties of coal fly ash: a global review. *Case Stud. Constr. Mater.*, 11, e00263. DOI: [10.1016/J.CSCM.2019.E00263](https://doi.org/10.1016/J.CSCM.2019.E00263).
- Brunauer S., Emmett P.H., Teller E., 1938. Adsorption of gases in multimolecular layers. *J. Am. Chem. Soc.*, 60, 309–319. DOI: [10.1021/ja01269a023](https://doi.org/10.1021/ja01269a023).
- Chowdhury Z.Z., Zain S.M., Khan R.A., Rafique R.F., Khalid K., 2012. Batch and fixed bed adsorption studies of lead (II) cations from aqueous solutions onto granular activated carbon derived from mangostana garcinia shell. *BioRes.*, 7, 2895–2915. DOI: [10.15376/biores.7.3.2895-2915](https://doi.org/10.15376/biores.7.3.2895-2915).
- Cobbina S.J., Duwiejuah A.B., Quainoo A.K., 2019. Single and simultaneous adsorption of heavy metals onto groundnut shell biochar produced under fast and slow pyrolysis. *Int. J. Environ. Sci. Technol.*, 16, 3081–3090. DOI: [10.1007/s13762-018-1910-9](https://doi.org/10.1007/s13762-018-1910-9).
- De Buyck P.-J., Van Hulle S.W.H., Dumoulin A., Rousseau D.P.L., 2021. Roof runoff contamination: a review on pollutant nature, material leaching and deposition. *Rev. Environ. Sci. Biotechnol.*, 20, 549–606. DOI: [10.1007/s11157-021-09567-z](https://doi.org/10.1007/s11157-021-09567-z).
- Dehghani M.H., Ahmadi S., Ghosh S., Othmani A., Osagie C., Meskini M., Alkafaas S.S., Malloum A., Khanday W.A., Jacob A.O., Gökkuş Ö., Oroke A., Chineme O.M., Karri R.R., Lima E.C., 2023. Recent advances on sustainable adsorbents for the remediation of noxious pollutants from water and wastewater: a critical review. *Arab. J. Chem.*, 16, 105303. DOI: [10.1016/j.arabjc.2023.105303](https://doi.org/10.1016/j.arabjc.2023.105303).
- Gkika D.A., Mitrpoulos A.C., Kyzas G.Z., 2022. Why reuse spent adsorbents? The latest challenges and limitations. *Sci. Total Environ.*, 822, 153612. DOI: [10.1016/j.scitotenv.2022.153612](https://doi.org/10.1016/j.scitotenv.2022.153612).
- Gong Y., Sun J., Sun S.-Y., Lu G., Zhang T.A., 2019. Enhanced desilication of high alumina fly ash by combining physical and chemical activation. *Metals*, 9, 411. DOI: [10.3390/MET9040411](https://doi.org/10.3390/MET9040411).
- Guo T., Yao S., Chen H., Yu X., Wang M., Chen Y., 2017. Characteristics and adsorption study of the activated carbon derived from municipal sewage sludge. *Water Sci. Technol.*, 76, 1697–1705. DOI: [10.2166/wst.2017.352](https://doi.org/10.2166/wst.2017.352).
- Guo X., Zhao Z., Gao X., Dong Y., Fu H., Zhang X., 2024. Study on the adsorption performance of modified high silica fly ash for methylene blue. *RSC Adv.*, 14, 21342–21354. DOI: [10.1039/D4RA04017A](https://doi.org/10.1039/D4RA04017A).
- Hosseini Asl S.M., Javadian H., Khavarpour M., Belviso C., Taghavi M., Maghsudi M., 2019. Porous adsorbents derived from coal fly ash as cost-effective and environmentally-friendly sources of aluminosilicate for sequestration of aqueous and gaseous pollutants: a review. *J. Cleaner Prod.*, 208, 1131–1147. DOI: [10.1016/J.JCLEPRO.2018.10.186](https://doi.org/10.1016/J.JCLEPRO.2018.10.186).
- Jiang X., Fan W., Li C., Wang Y., Bai J., Yang H., Liu X., 2019. Removal of Cr (VI) from wastewater by a two-step method of oxalic acid reduction-modified fly ash adsorption. *RSC Adv.*, 9, 33949–33956. DOI: [10.1039/C9RA05980F](https://doi.org/10.1039/C9RA05980F).
- Katara S., Kabra S., Sharma A., Hada R., Rani A., 2013. Surface modification of fly ash by thermal activation: a DR/FTIR study. *Int. Res. J. Pure Appl. Chem.*, 3, 299–307. DOI: [10.9734/IRJPAC/2013/4287](https://doi.org/10.9734/IRJPAC/2013/4287).
- Langmuir I., 1918. The adsorption of gases on plane surfaces of glass, mica and platinum. *J. Am. Chem. Soc.*, 40, 1361–1403. DOI: [10.1021/ja02242a004](https://doi.org/10.1021/ja02242a004).
- Mao L., Wu M., Zhu S., Wang X., Zhang J., Qin Y., 2024. Adsorption potential and mechanism of sludge-based activated carbon modified with fly ash for removal of heavy metals. *Sustainability*, 16, 2972. DOI: [10.3390/su16072972](https://doi.org/10.3390/su16072972).
- Marszałek A., 2022. Encapsulation of halloysite with sodium alginate and application in the adsorption of copper from rainwater. *Arch. Environ. Prot.*, 48, 75–82. DOI: [10.24425/aep.2022.140546](https://doi.org/10.24425/aep.2022.140546).
- Mushtaq F., Zahid M., Ahmad Bhatti I.A., Nasir S., Hussain T., 2019. Possible applications of coal fly ash in wastewater treatment. *J. Environ. Manage.*, 240, 27–46. DOI: [10.1016/j.jenvman.2019.03.054](https://doi.org/10.1016/j.jenvman.2019.03.054).
- Oktaviansyah I., Yuliwati E., Ariyanto E., 2024. Optimization of domestic wastewater treatment using a mixture of coconut shell activated carbon adsorbent and fly ash. *Sainmatika: Jurnal Ilmiah Matematika dan Ilmu Pengetahuan Alam*, 21 (2), 122–133. DOI: [10.31851/sainmatika.v21i2.16246](https://doi.org/10.31851/sainmatika.v21i2.16246).
- Olivier J.P., 1995. Modeling physical adsorption on porous and nonporous solids using density functional theory. *J. Porous Mater.*, 2, 9–17. DOI: [10.1007/BF00486565](https://doi.org/10.1007/BF00486565).
- Othmani A., Magdouli S., Senthil Kumar P., Kapoor A., Velayudhaperumal Chellam P., Gökkuş Ö., 2022. Agricultural waste materials for adsorptive removal of phenols, chromium (VI) and cadmium (II) from wastewater: a review. *Environ. Res.*, 204, 111916. DOI: [10.1016/j.envres.2021.111916](https://doi.org/10.1016/j.envres.2021.111916).
- Qiu Q., Jiang X., Lv G., Chen Z., Lu S., Ni M., Yan J., Deng X., 2018. Adsorption of heavy metal ions using zeolite materials of municipal solid waste incineration fly ash modified by microwave-assisted hydrothermal treatment. *Powder Technol.*, 335, 156–163. DOI: [10.1016/j.powtec.2018.05.003](https://doi.org/10.1016/j.powtec.2018.05.003).
- Regulation of the Minister of Maritime Economy and Inland Navigation of 12 July 2019 on substances particularly harmful to the aquatic environment and the conditions that must be met when discharging sewage into waters or soil, as well as when discharging rainwater or meltwater into waters or water facilities. *Journal of Laws* 2019, Item 1395 (Dz.U. 2019 poz. 1311, in Polish). Available at: [https://isap.sejm.gov.pl/isap.nsf/DocDetails.xsp?id=\\$WDU20190001311](https://isap.sejm.gov.pl/isap.nsf/DocDetails.xsp?id=$WDU20190001311).
- Singh N.B., Agarwal A., De A., Singh P., 2022. Coal fly ash: an emerging material for water remediation. *Int. J. Coal Sci. Technol.*, 9, 44. DOI: [10.1007/s40789-022-00512-1](https://doi.org/10.1007/s40789-022-00512-1).
- Sulyman M., Kucinska-Lipka J., Sienkiewicz M., Gierak A., 2021. Development, characterization and evaluation of composite adsorbent for the adsorption of crystal violet from aqueous solution: Isotherm, kinetics, and thermodynamic studies. *Arabian J. Chem.*, 14, 103115. DOI: [10.1016/j.arabjc.2021.103115](https://doi.org/10.1016/j.arabjc.2021.103115).
- Szymańska M., Nowicki P., 2023. Used filter cartridges as potential adsorbents of organic pollutants. *Water*, 15, 714. DOI: [10.3390/w15040714](https://doi.org/10.3390/w15040714).

- Tan I.A.W., Abdullah M.O., Lim L.L.P., Yeo T.H.C., 2017. Surface modification and characterization of coconut shell-based activated carbon subjected to acidic and alkaline treatments. *J. Appl. Sci. Process Eng.*, 4, 186–194. DOI: [10.33736/jaspe.435.2017](https://doi.org/10.33736/jaspe.435.2017).
- Tursi A., Chatzisyneon E., Chidichimo F., Beneduci A., Chidichimo G., 2018. Removal of endocrine disrupting chemicals from water: adsorption of bisphenol-A by biobased hydrophobic functionalized cellulose. *Int. J. Environ. Res. Public Health*, 15, 2419. DOI: [10.3390/ijerph15112419](https://doi.org/10.3390/ijerph15112419).
- Yao Z.T., Ji X.S., Sarker P.K., Tang J.H., Ge L.Q., Xia M.S., Xi Y.Q., 2015. A comprehensive review on the applications of coal fly ash. *Earth Sci. Rev.*, 141, 105–121. DOI: [10.1016/J.EARSCIREV.2014.11.016](https://doi.org/10.1016/J.EARSCIREV.2014.11.016).
- Zaimee M.Z.A., Sarjadi M.S., Rahman M.L., 2021. Heavy metals removal from water by efficient adsorbents. *Water*, 13, 2659. DOI: [10.3390/w13192659](https://doi.org/10.3390/w13192659).
- Zhang H., Husain T., 2021. Affordable water filtration technology for disinfection by-product control for small rural communities by using carbon extracted from local fly ash. *J. Miner. Mater. Charact. Eng.*, 9, 148–168. DOI: [10.4236/JMMCE.2021.92011](https://doi.org/10.4236/JMMCE.2021.92011).